THE JOURNAL OF BIOLOGICAL CHEMISTRY VOL. 285, NO. 16, pp. 11958–11965, April 16, 2010

Three Homologous Subunits Form a High Affinity Peptide-gated Ion Channel in *Hydra*[*]

Received for publication, August 26, 2009, and in revised form, January 20, 2010 Published, JBC Papers in Press, February 16, 2010, DOI 10.1074/jbc.M109.059998

Stefan Dürrnagel[‡], Anne Kuhn[§], Charisios D. Tsiairis[§], Michael Williamson[¶], Hubert Kalbacher[‖], Cornelis J. P. Grimmelikhuijzen[¶], Thomas W. Holstein[§], and Stefan Gründer[‡1]

From the [‡]Department of Physiology, RWTH Aachen University, D-52074 Aachen, Germany, the [§]Department of Molecular Evolution and Genomics, Heidelberg Institute of Zoology, D-69120 Heidelberg, Germany, the [¶]Center for Functional and Comparative Insect Genomics, Department of Biology, University of Copenhagen, DK-2100 Copenhagen, Denmark, and the [‖]Interfakultäres Institut für Biochemie, University of Tübingen, D-72074 Tübingen, Germany

Recently, three ion channel subunits of the degenerin (DEG)/epithelial Na^+ channel (ENaC) gene family have been cloned from the freshwater polyp *Hydra magnipapillata*, the *Hydra* Na^+ channels (HyNaCs) 2–4. Two of them, HyNaC2 and HyNaC3, co-assemble to form an ion channel that is gated by the neuropeptides Hydra-RFamides I and II. The HyNaC2/3 channel is so far the only cloned ionotropic receptor from cnidarians and, together with the related ionotropic receptor FMRFamide-activated Na^+ channel (FaNaC) from snails, the only known peptide-gated ionotropic receptor. The HyNaC2/3 channel has pore properties, like a low Na^+ selectivity and a low amiloride affinity, that are different from other channels of the DEG/ENaC gene family, suggesting that a component of the native *Hydra* channel might still be lacking. Here, we report the cloning of a new ion channel subunit from *Hydra*, HyNaC5. The new subunit is closely related to HyNaC2 and -3 and co-localizes with HyNaC2 and -3 to the base of the tentacles. Coexpression in *Xenopus* oocytes of HyNaC5 with HyNaC2 and -3 largely increases current amplitude after peptide stimulation and affinity of the channel to Hydra-RFamides I and II. Moreover, the HyNaC2/3/5 channel has altered pore properties and amiloride affinity, more similarly to other DEG/ENaC channels. Collectively, our results suggest that the three homologous subunits HyNaC2, -3, and -5 form a peptide-gated ion channel in *Hydra* that could contribute to fast synaptic transmission.

The DEG/ENaC[2] gene family contains ion channels that have a high selectivity for Na^+ ions and a rather high affinity for the diuretic amiloride (apparent $IC_{50} \sim 0.1–20\ \mu M$). In contrast to these conserved pore properties, activating stimuli and physiological functions of DEG/ENaC channels are strikingly diverse (1); family members from *Drosophila* are involved in the control of locomotion (2), the liquid clearance from the trachea (3), and in the detection of pheromones (4) and salt (5); members from *Caenorhabditis elegans* form mechanosensitive ion channels (6); FaNaC from snails is a peptide-gated ion channel (7); and the epithelial Na^+ channel (ENaC) and acid-sensing ion channels family members from mammals mediate Na^+ reabsorption (8) and are proton-gated ion channels (9), respectively. The functions of many other DEG/ENaC channels are still unknown.

Recently, three DEG/ENaC subunits have been cloned from the freshwater polyp *Hydra* (10). These subunits, HyNaC2-4, were the first DEG/ENaC channels from Cnidaria, which is an ancient phylum, where the first nervous systems are supposed to have evolved. A fourth HyNaC gene, *hynac1*, is probably a pseudogene (10). Moreover, it was shown that HyNaC2 and HyNaC3 co-assemble to form a heteromeric ion channel gated by Hydra-RFamides I and II (10), which are neuropeptides isolated from the nervous system of *Hydra* (11). The mRNA of HyNaC2 and HyNaC3 was localized by *in situ* hybridization to the base of the tentacles (10), in close proximity to the nerve cells that express the preprohormone gene that encodes Hydra-RFamides (12), suggesting that these neuropeptides are the natural ligand of the HyNaC2/3 channel. Although the precise location of HyNaCs is not known, it was proposed that they are expressed at the basolateral face of epitheliomuscular cells, and it was speculated that release of Hydra-RFamides leads to tentacle contractions, possibly during feeding of the animals (10).

The presence of a peptide-gated channel in the primitive nervous system of a cnidarian suggests that neuropeptides were already used for fast neurotransmission in ancient nervous systems. It also indicates that peptide gating is an ancient feature of DEG/ENaC channels and that this feature has been preserved during evolution in various members of the Protostomia, such as snails, but probably been lost in the Deuterostomia, such as mammals, where other ligands have replaced the peptide ligands.

The HyNaC2/3 channel has pore properties, like a low Na^+ selectivity and a low amiloride affinity ($IC_{50} \sim 500\ \mu M$), which are different from other channels of the DEG/ENaC gene family (10). These results suggest either that a high Na^+ selectivity and a high amiloride affinity are not ancient features of the gene family or that a component of the native *Hydra* channel is still lacking.

* This work was supported by the Deutsche Forschungsgemeinschaft SFB 488 (to T. W. H.), SFB 685 (to H. K.), the Danish Research Agency (to C. J. P. G.), and the Heidelberg Cluster of Excellence CellNetworks (to C. D. T.).

The nucleotide sequence(s) reported in this paper has been submitted to the DDBJ/GenBank™/EBI Data Bank with accession number(s) FN257513.

[1] To whom correspondence should be addressed: Dept. of Physiology, RWTH Aachen University, Pauwelsstrasse 30, D-52074 Aachen, Germany. Tel.: 49-241-80-88800; Fax: 49-241-80-82434; E-mail: sgruender@ukaachen.de.

[2] The abbreviations used are: DEG, degenerin; ENaC, epithelial Na^+ channel; BLINaC, brain-liver-intestine Na^+ channel; HA, hemagglutinin; FaNaC, FMRFamide-activated Na^+ channel; HyNaC, Hydra Na^+ channel; RFamide, Arg-Phe-NH_2; RACE, rapid amplification of cDNA ends.

Here, we report the cloning of a new ion channel subunit from *Hydra*, HyNaC5. *In situ* hybridization analysis and functional analysis of HyNaC5 suggest that the three homologous subunits HyNaC2, -3, and -5 form a high affinity peptide-gated ion channel in *Hydra*. Moreover, preliminary results suggest that this channel could be involved in the coordination of the feeding reaction of *Hydra*.

EXPERIMENTAL PROCEDURES

Cloning of HyNaC5—Several partial sequences for a protein showing sequence homology to HyNaCs were identified from the on-line *Hydra* expressed sequence tag data base and used to design primers for rapid amplification of 3′-cDNA ends (RACE). Using the Smart RACE cDNA amplification kit (Clontech), two rounds of 3′-RACE were performed with cDNA prepared from poly(A)$^+$ RNA, isolated from adult one-day starved budding stage *Hydra magnipapillata* (strain 105). Full-length HyNaC5 was assembled from expressed sequence tags and 3′-RACE products. For expression studies in *Xenopus* oocytes, the entire coding sequence of HyNaC5 was amplified by PCR from cDNA of whole *Hydras* and subcloned. The clone was entirely sequenced to exclude PCR errors. The consensus sequence of HyNaC5 was assembled from the expressed sequence tags and several independent PCR products. This sequence data has been submitted to the DDBJ/EMBL/GenBank^{TM} databases under accession number FN257513.

In Situ Hybridization—A 1,435-bp fragment from the coding part of HyNaC5 cDNA was subcloned in the vector pBluescript KS. Whole mount ISH was carried out as described previously (13) by using BMP Purple as substrate for the antibody-conjugated alkaline phosphatase, except that blocking of the animals was performed in monoclonal antibody/1× blocking reagent (Roche Applied Science) and that the alkaline phosphatase-conjugated anti-digoxygenin Fab fragments (Roche Applied Science) were diluted 1:4,000. Two different antisense probes of 810 and 1,435 bp, respectively, were used at concentrations of 0.08–0.16 ng/μl for 60 h. Both probes applied alone or together resulted in the same localization pattern, a combination of both probes yielding a stronger signal than the single probes. Performing ISH with the corresponding sense riboprobes did not display any staining.

Analysis of the Feeding Reaction of Hydra—Five animals of the species *H. magnipapillata* (wild-type strain 105) were placed in 10 ml of *Hydra* medium (1.0 mM Tris-HCl, 1.0 mM $NaHCO_3$, 0.1 mM KCl, 0.1 mM $MgCl_2$, and 1.0 mM $CaCl_2$) or *Hydra* medium supplemented with 100 μM amiloride. Once they were relaxed in the new medium, glutathione was added to a final concentration of 10 μM at time 0. Every 30 s, we recorded the number of animals moving their tentacles as a response to the application of glutathione. The experiments were repeated four times. Additional experiments were performed with *Hydra oligactis* without finding any differences (data not shown).

Electrophysiology—Synthesis of cRNA, maintenance of *Xenopus laevis* oocytes and recordings of whole cell currents were done as described previously (14). For coexpression of HyNaC subunits, we injected equal amounts of cRNAs of the individual subunits; the total amount was 0.3–8 ng. To avoid artifacts due to tachyphylaxis, for the experiments determining the relative inward currents with different monovalent cations (see Fig. 6) and different blockers (see Fig. 7), we activated the HyNaC2/3/5 heteromer two times before varying the concentration of the cations or blockers, respectively. To further reduce the impact of tachyphylaxis in both experiments, the sequence of the inhibitors or cations was varied. Oocytes from at least two different frogs were used, except for determination of apparent amiloride affinity of HyNaC2/3, for which oocytes from one frog were used.

Determination of Surface Expression—The hemagglutinin (HA) epitope (YPYDVPDYA) of influenza virus was inserted in the extracellular loop of HyNaC2 between residues Phe^{124} and Asp^{125}. HyNaC2/3/5 containing tagged HyNaC2 had similar apparent peptide affinity as HyNaC2/3/5 containing untagged HyNaC2 and current amplitude of HyNaC2/3 containing tagged HyNaC2 was >10-fold increased by coexpressing HyNaC5 (results not shown).

Oocytes were injected with ~3 ng cRNA of each subunit, and surface expression was determined as described previously (15). Briefly, oocytes expressing HyNaCs were placed for 30 min in ND96 with 1% bovine serum albumin to block unspecific binding, incubated for 60 min with 0.5 μg/ml of rat monoclonal anti-HA antibody (3F10, Roche Applied Science), washed extensively with ND96/1% bovine serum albumin, and incubated for 60 min with 2 μg/ml of horseradish peroxidase-coupled secondary antibody (goat anti-rat Fab fragments, Jackson ImmunoResearch Laboratories). Oocytes were washed six times with ND96/1% bovine serum albumin and three times with ND96 without bovine serum albumin. All steps were performed on ice. Oocytes were then placed individually in wells of microplates, and luminescence was quantified in a Berthold Orion II luminometer (Berthold Detection Systems; Pforzheim, Germany). The chemiluminescent substrates (50 μl of Power Signal ELISA; Pierce) were automatically added, and luminescence was measured after 2 s for 5 s. Relative light units/s were calculated as a measure of surface-expressed channels. The results are from two independent experiments with oocytes from two different frogs. Eight oocytes were analyzed for each experiment and each condition.

RESULTS AND DISCUSSION

Cloning of HyNaCs from H. magnipapillata—We isolated a new cDNA with high homology to HyNaCs (Fig. 1) from *H. magnipapillata* cDNA; we named the corresponding protein HyNaC5. The predicted amino acid sequence of HyNaC5 is shown together with the sequences of HyNaC2–4 in Fig. 1*A*. The degree of amino acid sequence identities between HyNaC5 and HyNaC2–4 ranges from 28–44%; the closest relative is HyNaC2 (Fig. 1*B*). Thus, sequence identities between different HyNaCs are similar to sequence identities between the three subunits of the epithelial Na^+ channel, ENaC (16). The open reading frame of the HyNaC5 cDNA codes for a protein of 473 amino acids with a predicted molecular mass of ~55 kDa. HyNaC5 shows the structural hallmarks of the DEG/ENaC gene family: two hydrophobic transmembrane domains, short N and C termini, and a large extracellular loop containing 12

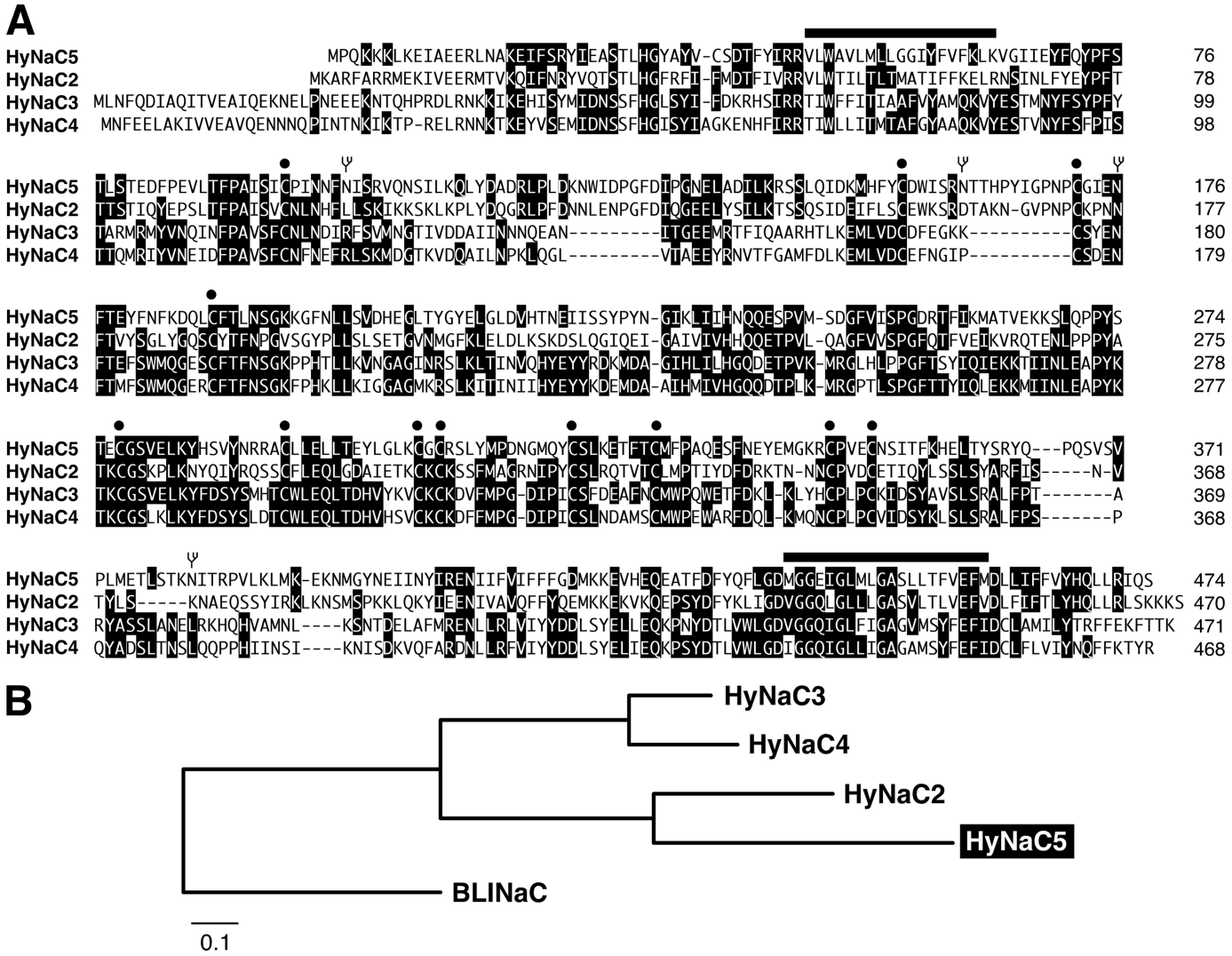

FIGURE 1. *A*, sequence alignment of HyNaC5 with HyNaC2–4. Amino acids showing a high degree of identity are shown as *white letters on a black background*. The putative positions of transmembrane domains are indicated by *bars*, conserved cysteines are indicated by *circles*, and consensus sequences for *N*-linked glycosylation in HyNaC5 are indicated by *branched symbols*. Accession numbers are as follows: HyNaC2, AM393878; HyNaC3, AM393880; HyNaC4, AM393881; and HyNaC5, FN257513. *B*, *phylogram* illustrating the relationship of HyNaCs. Amino acid sequences of HyNaC2–5 and rat BLINaC were aligned, and the tree for the phylogram was established by Neighbor Joining with ClustalX; highly divergent sequences at the N and C termini had been deleted. Branch lengths are proportional to the evolutionary distance. BLINaC is a related channel (10) that was included for comparison; the accession number of rat BLINaC is Y19034.

conserved cysteines between the two hydrophobic domains (Fig. 1*A*). A topology with two transmembrane domains, a large ectodomain, and short intracellular termini is common to all DEG/ENaC subunits (1).

Expression Pattern of hynac5—Whole mount *in situ* hybridization for *hynac5* revealed expression at the base of the tentacles (Fig. 2*A*), most likely in epitheliomuscular cells. During budding, *hynac5* is expressed at the sites of tentacle formation, immediately before the first tentacle bumps appear (Fig. 2*G*). Thus, the expression pattern of *hynac5* is very similar to the expression patterns of *hynac2* and *hynac3* (Fig. 2) (10), suggesting that the three genes are coexpressed in *Hydra* cells.

A more careful comparison, however, reveals subtle differences in the expression pattern of the three genes. Although *hynac 2* and *hynac3* are uniformly expressed at the tentacle base (Fig. 2, *B* and *C*), *hynac5* expression is strongest at the oral site of each tentacle base with a gradient toward the aboral site (Fig. 2*A* and Fig. 3*A*). By comparison, *hynac4* expression exhibits a strong restriction to the aboral site of the tentacles (Fig. 3*B*) (10). The mutually exclusive expression patterns of *hynac4* and *hynac*5 at the base of the tentacles suggest a different function for HyNaC4 and HyNaC5.

Previously, it was speculated that activation of HyNaCs leads to tentacle contractions during the "feeding reaction" of *Hydra* (10). The feeding reaction is induced by physical contact with a prey animal and characterized by an upward movement and contraction of the tentacles, which brings the prey close to the mouth (17). Perhaps HyNaC4 and HyNaC5 have distinct roles in the coordination of this feeding behavior.

HyNaC5 Strongly Increases Current Amplitude of the HyNaC2/3 Heteromer—We investigated the functional properties of HyNaC5 by expression in *Xenopus* oocytes; cRNAs coding for HyNaC2–5 were injected in oocytes either alone or in combination. Oocytes expressing HyNaC5 alone or in combination with one other HyNaC subunit (2, 3, or 4) could not be activated by any of the four Hydra-RFamides (I–IV; Fig. 4*A*). In contrast

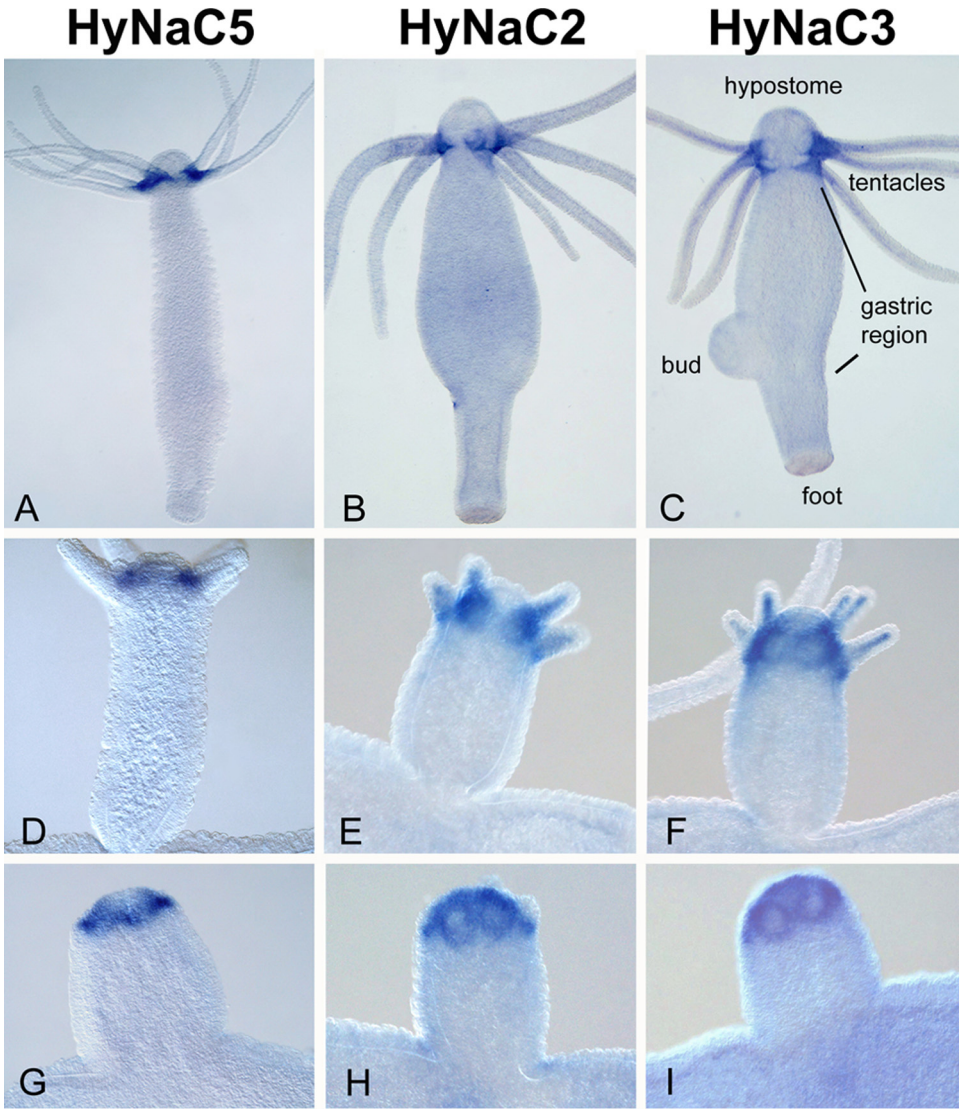

FIGURE 2. ***hynac5* is expressed at the base of the tentacles.** Whole mount *in situ* hybridization reveals strong expression of *hynac5* transcripts at the tentacle base in adult animals (*A*) and buds (*D* and *G*). By comparison *hynac2* and *hynac3* transcripts are uniformly distributed (*B* and *C*). During bud formation, *hynac5* transcripts appear as soon as tentacles begin to appear (*G*) similar to *hynac2* and *hynac3* (*E* and *F*, and *H* and *I*). Expression of *hynac5* is strongest at the *upper side* (oral) of the tentacles (*A*); primary magnifications are 4× (*A–C*) and 20× (*D–I*).

and as previously reported (10), oocytes coexpressing HyNaC2 and -3 exhibited a robust current after stimulation with Hydra-RFamide I (Fig. 4*A*) and II (data not shown); current amplitudes were usually in the range of a few μA. Oocytes expressing HyNaC5 in addition to HyNaC2 and -3 could also be activated by RFamides I and II and showed dramatically increased current amplitudes compared with oocytes coexpressing only HyNaC2 and -3: current amplitudes of oocytes expressing HyNaC2, -3, and -5 were so large (>50 μA) that they were above the capacity of our amplifier (Fig. 4*A*, *left panel*). A quantitative comparison with oocytes, which had been injected with 25-fold diluted RNA, and half-maximal peptide concentrations (see below) revealed a 16-fold increase in the peak current amplitude of HyNaC2/3/5 compared with HyNaC2/3 ($p \ll 0.01$; Fig. 4*A*, *right panel*), strongly suggesting that HyNaC5 was incorporated in the channel complex to form a HyNaC2/3/5 heteromer. Recently, the crystal structure of an acid-sensing ion channel revealed a number of three subunits in the functional channel (18). Because acid-sensing ion channels are close relatives of HyNaCs in the DEG/ENaC gene family (10), it is reasonable to assume that functional HyNaCs are also composed of three subunits, suggesting a 1:1:1 ratio for the HyNaC2, -3, and -5 subunits in the functional complex. In the remainder of this study, we usually injected 25-fold diluted cRNAs of HyNaC2/3/5 to get current amplitudes in the range of 1–30 μA. Oocytes coexpressing HyNaC5 together with HyNaC2 and -4 could also be activated by Hydra-RFamides I and II; current amplitudes were much smaller than for the HyNaC2/3/5 heteromer, however (Fig. 4*A*), suggesting that although HyNaC4 is closely related to HyNaC3 (Fig. 1*B*) it cannot efficiently replace it in the heteromeric complex.

Fig. 4*B* shows representative current traces of oocytes expressing HyNaC2, -3, and -5. Similar to HyNaC2/3 channels (10) and FaNaC (7), HyNaC2/3/5 heteromers desensitized incompletely: a rapidly declining peak amplitude was followed by a sustained current; the ratio between peak and sustained current was variable. A second application of the ligand induced currents with significantly smaller amplitudes than the first application. Further applications of the ligand, however, induced currents with amplitudes comparable with the second application (Fig. 4*B*).

HyNaC5 Strongly Increases the Current through Surface-expressed HyNaCs—Increased current amplitudes of the HyNaC2/3/5 heteromer compared with the HyNaC2/3 heteromer (Fig. 4*A*) can be due to increased surface expression and/or increased current through surface-expressed channels. To differentiate between these possibilities, we compared the expression of the two heteromers at the oocyte surface. We inserted an HA epitope into the extracellular loop of HyNaC2 and used a monoclonal anti-HA antibody and a luminescence assay to compare the surface expression of HA-tagged channels (15). Luminescence was not significantly different ($p = 0.3$) between oocytes expressing the HyNaC2/3/5 heteromer and oocytes expressing the HyNaC2/3 heteromer (Fig. 4*C*). For oocytes expressing the heteromers, luminescence was, however, significantly larger than for oocytes expressing HyNaC2-HA alone ($p \leq 0.01$),

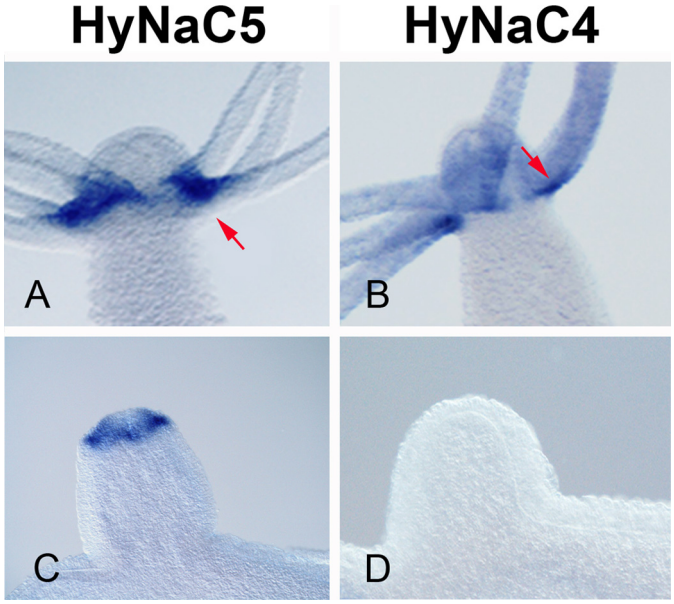

FIGURE 3. ***hynac5* and *hynac4* show complementary expression patterns.** *hynac5* is expressed at the oral site of the tentacle bases (*A*) and in early bud (*C*), whereas *hynac4* is expressed at the aboral site of the tentacles (*B*); it also lacks any expression in early bud stages. *Arrows* indicate the different expression zones of both genes; primary magnifications are 20× (*A–C*).

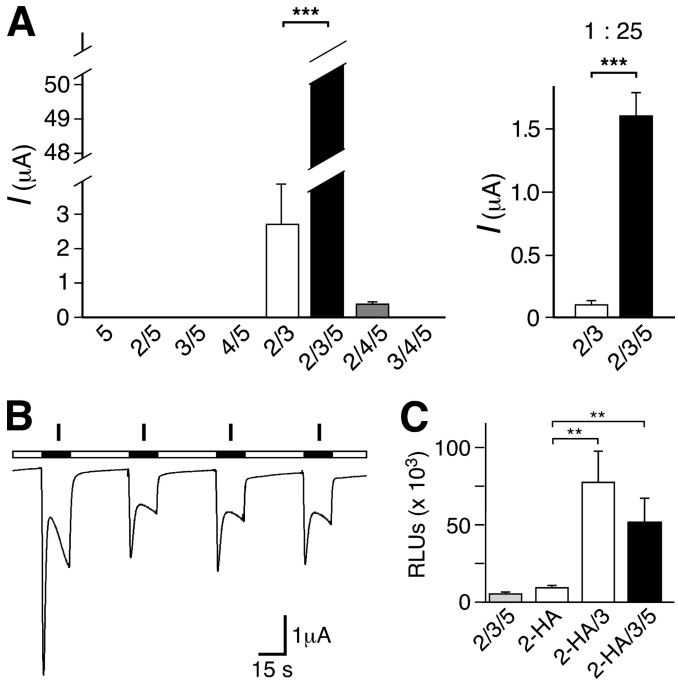

FIGURE 4. *A*, HyNaC5 potently increases the current amplitude of the HyNaC2/3 heteromer. *Left*, *bar graphs* illustrating the whole oocyte current amplitude after coexpression of different combinations of HyNaC subunits; HyNaCs were activated with 30 μM Hydra-RFamide I. For each condition, a total of ~8 ng cRNA had been injected in oocytes. Note that the amplitude for HyNaC2/3/5 was >50 μA and therefore only a lower limit of the amplitude can be given. *Error bars* represent S.E.; for HyNaC2/3/5, the S.E. could not be calculated. $n = 10$ oocytes. *Right*, bar graphs illustrating current amplitude of oocytes coexpressing HyNaC2/3 or HyNaC2/3/5; a total of ~0.3 ng cRNA had been injected. Both channels were activated with a concentration of Hydra-RFamide II eliciting half-maximal response: HyNaC2/3 with 33 μM and HyNaC2/3/5 with 0.35 μM. ***, $p < 0.001$. *B*, representative current traces for the HyNaC2/3/5 heteromer. Repeated activation of HyNaC2/3/5 with Hydra-RFamides led to decreased response between the first and second application; in the example shown, 30 μM Hydra-RFamide I was used. cRNA for HyNaCs 2, 3, and 5 was diluted 25-fold (a total of 0.3 ng/oocyte). *C*, HyNaC5 does not increase surface expression of the HyNaC2/3 heteromer. Surface expression of HyNaC2 and HyNaC2/3 in comparison to HyNaC2/3/5 (mean ± S.E.); only the HyNaC2 subunit was HA-tagged. Oocytes injected with untagged HyNaC2/3/5 served as a control (*first column*). The results are expressed as relative light units (*RLUs*)/oocyte/s ($n = 16$). **, $p \leq 0.01$.

for which luminescence was not significantly above background ($p = 0.2$; Fig. 4*C*).

Assuming a number of three subunits in a functional HyNaC (18), in the 2/3/5 channel only one subunit per channel was tagged, whereas in the 2/3 channel either one or two subunits were tagged, depending on the subunit stoichiometry (2/3/3 or 2/2/3). Therefore, in the case of a 2/2/3 channel, our assay would underestimate the surface expression of the 2/3/5 channel relative to the 2/2/3 channel by a factor of 2. Even in this case, however, the difference in surface expression (at most 2-fold) cannot account for the 16-fold difference in current amplitude (Fig. 4*A*). Thus, HyNaC5 predominantly increases the current through surface-expressed channels. This result suggests that the HyNaC2/3 heteromer either has a small single channel amplitude or that Hydra-RFamides are partial agonists at this channel, leading to a low open probability.

Similar to HyNaC2/3/5, ENaC is also composed of three homologous subunits (α, β, and γ) (16). ENaCs composed of only two different subunits (αβ or αγ), are also active but produce much smaller currents than those composed of three different subunits (αβγ), similar to HyNaCs composed of only two (2/3) different subunits. In contrast to HyNaC2/3, however, the low amplitude of αβ and αγ ENaCs is primarily due to low surface expression (19).

HyNaC5 Changes the Properties of the HyNaC2/3 Heteromer—Similar to HyNaC2/3, HyNaC2/3/5 was activated by Hydra-RFamides I and II. For both peptides, the affinity of HyNaC2/3/5 was increased ~100-fold compared with HyNaC2/3 (Fig. 5): half-maximal activation was obtained with 4.8 ± 2.0 μM (mean ± S.E.; eight oocytes) Hydra-RFamide I and 0.34 ± 0.08 μM (eight oocytes) Hydra-RFamide II compared with 326 ± 108 μM and 38 ± 13 μM (four oocytes, each), respectively, for HyNaC2/3. In each case, the concentration response curve could be well fitted assuming a single population of channels, suggesting that most of the channels in oocytes coexpressing HyNaC2, -3, and -5 were of a single type (2/3/5). Hill coefficients were similar for HyNaC2/3/5 and HyNaC2/3 (0.9 ± 0.1 compared with 0.8 ± 0.1 for Hydra-RFamide I, $p = 0.6$, and 1.8 ± 0.2 compared with 1.7 ± 0.4 for Hydra-RFamide II, $p = 0.8$, respectively; $n = 8$ for HyNaC 2/3/5 and $n = 4$ for HyNaC 2/3).

Previous evidence suggested that Hydra-RFamides activate HyNaC2/3 directly and not by a second messenger cascade (10). Activation of HyNaC2/3/5 with a strongly increased affinity for Hydra-RFamides further confirms that the binding sites for Hydra-RFamides are on HyNaCs and that these peptides directly activate HyNaCs.

In oocytes expressing the HyNaC2/3/5 heteromer (dilution, 1:25), high concentrations (50 μM) of Hydra-RFamides III and IV also elicited a tiny current (<0.1 μA; data not shown), suggesting that these peptides are agonists at this channel with a very low affinity. Hydra-RFamides III and IV did not activate other subunit combinations, also containing HyNaC4. We speculate that a related channel, perhaps containing HyNaC4

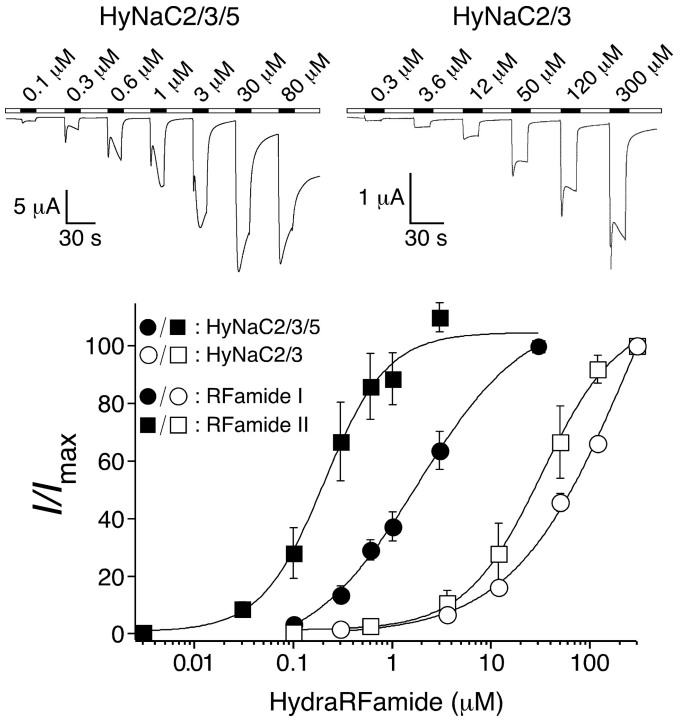

FIGURE 5. **HyNaC5 strongly increases apparent affinity for Hydra-RFamides.** *Top*, representative current traces of whole oocytes either expressing HyNaC2 and -3 or HyNaC2, -3, and -5; channels were activated with Hydra-RFamide I. *Bottom*, concentration-response curves for HyNaC2/3 (*open symbols*) and HyNaC2/3/5 (*closed symbols*), each with Hydra-RFamides I (*circles*) and II (*squares*). *Error bars* represent S.E., and lines were fitted to the Hill function. Current amplitudes were normalized to the amplitude obtained with the highest concentration of the ligand (I_{max}) ($n = 8$ for HyNaC2/3/5 and $n = 4$ for HyNaC 2/3).

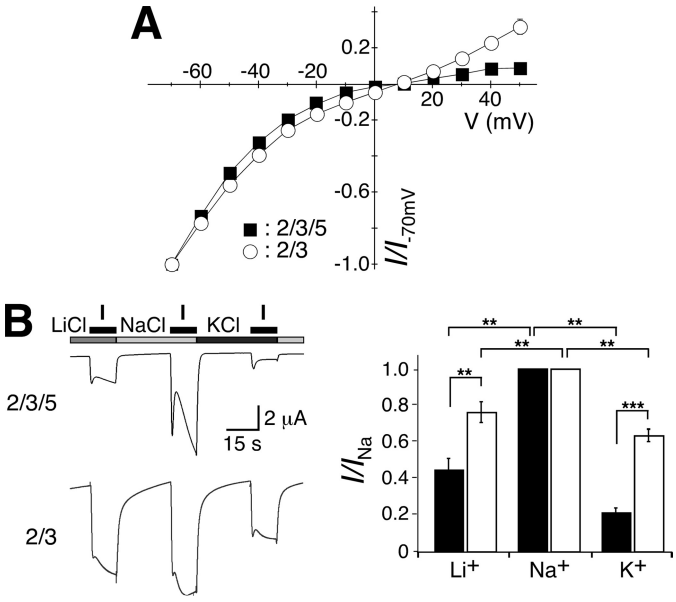

FIGURE 6. **Ion selectivity of HyNaC2/3/5.** *A*, the HyNaC5 subunit does not change reversal potentials. Channels were activated with 30 μM (HyNaC2/3) or 0.3 μM Hydra-RFamide I (HyNaC2/3/5), respectively, and reversal potentials measured by stepping to the indicated holding potentials for 3 s. *B*, the HyNaC5 subunit decreases currents carried by K^+. *Left*, representative current traces of whole oocytes either expressing HyNaC2 and -3 or HyNaC2, -3, and -5. Channels were activated in the presence of different monovalent cations. *Right*, *bar graphs* illustrating the amplitude of the Li^+ and K^+ current relative to the Na^+ current; *black bars* represent HyNaC2/3/5, *white bars* HyNaC2/3. *Error bars* represent S.E. (12 oocytes); HyNaCs were activated with 30 μM (HyNaC2/3) or 0.3 μM Hydra-RFamide I (HyNaC2/3/5), respectively. In the presence of HyNaC5, amplitudes of Li^+ and K^+ currents were significantly reduced relative to the amplitude of the Na^+ current. **, $p < 0.01$; ***, $p < 0.001$, two-tailed *t* test.

in combination with other HyNaC subunits not yet identified, is the high affinity receptor for Hydra-RFamides III and IV.

Reversal potentials in standard bath solution were not significantly different between HyNaC2/3/5 and HyNaC2/3 (10.1 ± 1.2 mV compared with 8.6 ± 3.5 mV; $n = 8$; $p = 0.69$; Fig. 6*A*), indicating that the permeability ratio P_{Na}/P_K is similar for the two channels. The inward rectification of HyNaC2/3/5, however, suggests that for HyNaC2/3/5 outward K^+ currents are less well conducted than for HyNaC2/3. We further investigated ion permeability by replacing all extracellular Na^+ by Li^+ or K^+ and measuring the amplitude of inward currents at −70 mV. In the case of HyNaC2/3/5, inward currents with K^+ and Li^+ as the main charge carrier were significantly smaller than Na^+ currents ($p < 0.01$; Fig. 6*B*). This relative current reduction was especially prominent for K^+ and is consistent with the inward rectification observed with the *I*/*V* curves. In the case of HyNaC2/3, amplitudes of inward K^+ and Li^+ currents were also significantly smaller than Na^+ currents, but the reduction in relative amplitude was smaller than for HyNaC2/3/5 ($p < 0.01$; Fig. 6*B*). A reduced K^+ permeability, despite similar permeability ratios P_{Na}/P_K, would be expected when for example K^+ ions permeate more slowly through the HyNaC2/3/5 than through the HyNaC2/3 pore (20). Together, these results show that the ion pore of HyNaC2/3/5 has slightly different permeability properties than the HyNaC2/3 pore.

In addition to a low selectivity for monovalent cations, the HyNaC2/3 pore is characterized by a low apparent affinity for the open channel blocker amiloride (10), which is also uncommon for DEG/ENaC channels. We confirmed that for HyNaC2/3 the IC_{50} for amiloride is ~500 μM (540 ± 160 μM; five oocytes; Fig. 7*A*). In contrast, for HyNaC2/3/5 the IC_{50} for amiloride was significantly reduced (122 ± 9 μM; $p = 0.02$; six oocytes; Fig. 7*A*). As FaNaC is not only activated but also blocked by its peptide ligand, FMRFamide (21), we wondered whether the low apparent amiloride affinity of HyNaCs might be due to a competition with Hydra-RFamides at the rather high peptide concentrations (30 μM) used to determine amiloride affinity. However, even with a 100-fold lower concentration of the peptide (0.3 μM), apparent amiloride affinity of HyNaC2/3/5 was not significantly increased (IC_{50} = 98 ± 18 μM; $p = 0.2$; six oocytes; Fig. 7*A*), showing that Hydra-RFamides do not strongly compete with amiloride. Of note, at low concentrations (1 μM) amiloride slightly increased HyNaC current amplitudes. An increased open probability by amiloride has previously also been noted for FaNaC (22, 23). Finally, we compared the inhibition of HyNaC2/3 and HyNaC2/3/5 by 100 μM of the two amiloride analogs benzamil and phenamil. Both blockers more potently blocked HyNaC2/3/5 than HyNaC2/3 ($p < 0.05$; Fig. 7*B*). This increased apparent affinity was highly significant for benzamil, for which 100 μM blocked almost 90% of the current. The increased apparent affinity for open channel blockers further support the conclusion that HyNaC5 is incorporated into the HyNaC2/3 channel complex and contributes to its ion pore.

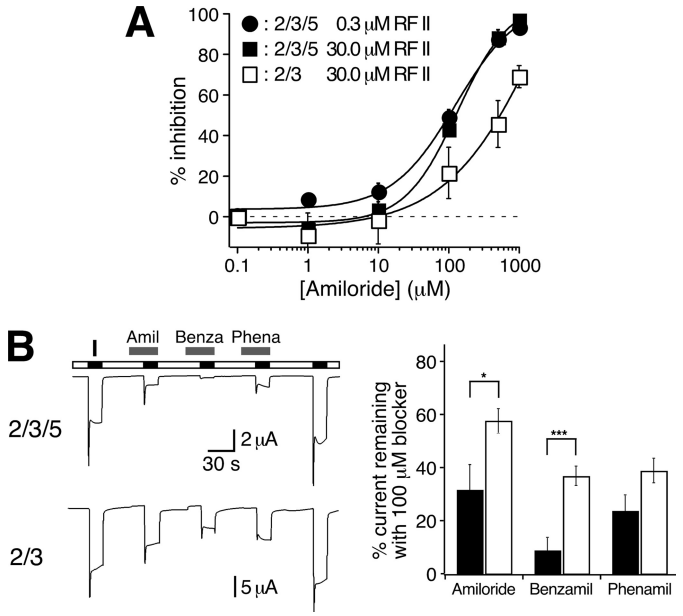

FIGURE 7. **HyNaC5 increases the apparent affinity for amiloride and amiloride analogs.** *A*, concentration response curve for the inhibition of HyNaC currents by amiloride. Curves were determined with 0.3 μM (HyNaC2/3/5) and 30 μM Hydra-RFamide II (HyNaC2/3 and HyNaC2/3/5), respectively (n = five oocytes for HyNaC2/3 and n = 6 oocytes for HyNaC2/3/5). *B*, *left*, representative current traces of whole oocytes either expressing HyNaC2 and -3 or HyNaC2, -3, and -5. Channels were activated in the presence of different blockers (100 μM). *Right*, *bar graphs* illustrating the current remaining in the presence of the respective blockers; *black bars* represent HyNaC2/3/5, *white bars* HyNaC2/3. Before and after application of the blockers, channels were activated without blockers; the mean value of these two measurements was used to normalize the currents obtained in the presence of the blockers. *Error bars* represent S.E. (six oocytes); HyNaCs were activated with 30 μM (HyNaC2/3) or 1 μM Hydra-RFamide I (HyNaC2/3/5), respectively. In the presence of HyNaC5, amiloride (*Aml*) and benzamil (*Benza*) blocked significantly more current, suggesting an increased affinity for these blockers. *, $p < 0.05$; ***, $p < 0.001$, two-tailed t test. *Phena*, phenamil.

Amiloride Delays the Feeding Reaction of Hydra—In situ hybridization suggested that HyNaCs might contribute to the feeding reaction of *Hydra*. We tried to support this hypothesis by investigating the feeding reaction in the presence of amiloride in the medium. The feeding reaction can be induced by glutathione (17). After addition of glutathione (10 μM final concentration), *Hydras* responded quickly by moving their tentacles, contracting them and bringing them to their mouth. When the animals were in a medium containing 100 μM amiloride, however, the initiation of tentacles movement was significantly delayed ($p < 0.05$; Fig. 8). Moreover, the movements did not lead to the characteristic contraction of the tentacles pointing them to the mouth. Similarly, the natural catching reaction after exposing *Hydra* to *Artemia* shrimps was inhibited by 100 μM amiloride (data not shown). These effects of amiloride were reversible; when animals were brought back to a medium without amiloride, they could feed on *Artemia* like the untreated ones and responded properly to glutathione by initiating the feeding reaction. Amiloride did not affect the general behavior of the animal; animals were still able to contract and move in the medium. However, they were unable to perform the coordinated movements of the tentacles associated with feeding reflex, suggesting the potential importance of amiloride-sensitive ion channels for the feeding reaction.

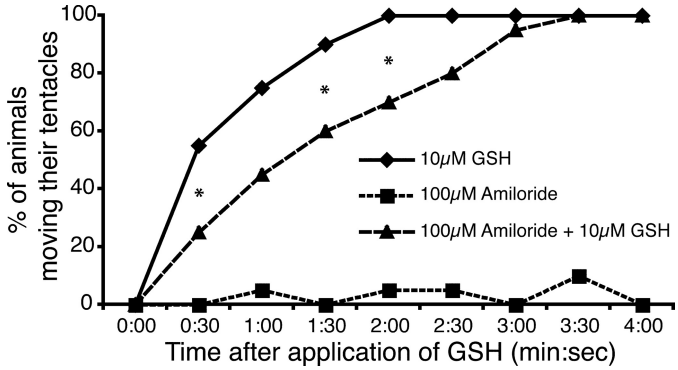

FIGURE 8. **Amiloride delays the glutathione induced feeding response.** *H. magnipapillata* were relaxed in plain medium or medium containing 100 μM amiloride. At time 0, glutathione was added to a final concentration of 10 μM. Every 30 s, the number of animals moving their tentacles was recorded. A statistically significant delay in the response to glutathione (*GSH*) was detected in the presence of amiloride. The calculated p value is < 0.05 as indicated (by an *asterisk*), whereas it is 0.06 for the time point 1:00.

Brief EPSPs with short synaptic delay have been recorded from the motor giant axon of the jellyfish *Aglantha digitale* (24), providing evidence for fast neurotransmission in Cnidaria. Recently genomic analysis indeed identified 11 ionotropic glutamate receptor subunits in the genome of the cnidarian *Nematostella vectensis* (25), suggesting that they could mediate fast transmission in *Nematostella*. In addition, the existence in cnidarians of channels from the nicotinic acetylcholine receptor/$GABA_A$ superfamily has been proposed (20); molecular evidence for such channels is so far lacking. Our results show that HyNaC2/3/5 form a peptide-gated ion channel and it should be considered that peptid-gated channels of the DEG/ENaC gene family contribute to fast neurotransmission in cnidarians.

The related FMRFamide-gated FaNaC has been localized to the membrane of snail neurons (26) and the properties of the endogenous current of those neurons match well with the properties of the recombinant FaNaC expressed in heterologous systems (7, 22, 27), showing that FaNaC carries a fast excitatory current in snail neurons. Defining more clearly the role of HyNaC for fast transmission in *Hydra* similarly requires, in the future, the electrophysiological characterization of the endogenous channel and localization of HyNaCs by immunocytochemistry.

Given the fact that HyNaC is the only cloned ionotropic receptor of cnidarians, its rather complicated architecture with three different subunits is remarkable. Moreover, each subunit makes a specific contribution to the overall properties of the channel. HyNaC5 for example, as shown in this study, probably contributes to the ligand-binding domain and to the precise structure of the channel pore. This situation is reminiscent of the ENaC (28), an evolutionary recent channel from mammals. Thus, some features of (DEG)/ENaC channels that seem highly evolved are shared by HyNaC and may have been present already in ancestral channels of this gene family. It can be expected that the investigation of HyNaCs will yield further insights into ancient properties and the evolution of the DEG/ENaC gene family.

Acknowledgment—We thank M. Pusch for helpful discussions.

REFERENCES

1. Kellenberger, S., and Schild, L. (2002) *Physiol. Rev.* **82,** 735–767
2. Ainsley, J. A., Pettus, J. M., Bosenko, D., Gerstein, C. E., Zinkevich, N., Anderson, M. G., Adams, C. M., Welsh, M. J., and Johnson, W. A. (2003) *Curr. Biol.* **13,** 1557–1563
3. Liu, L., Johnson, W. A., and Welsh, M. J. (2003) *Proc. Natl. Acad. Sci. U.S.A.* **100,** 2128–2133
4. Lin, H., Mann, K. J., Starostina, E., Kinser, R. D., and Pikielny, C. W. (2005) *Proc. Natl. Acad. Sci. U.S.A.* **102,** 12831–12836
5. Liu, L., Leonard, A. S., Motto, D. G., Feller, M. A., Price, M. P., Johnson, W. A., and Welsh, M. J. (2003) *Neuron* **39,** 133–146
6. O'Hagan, R., Chalfie, M., and Goodman, M. B. (2005) *Nat. Neurosci.* **8,** 43–50
7. Lingueglia, E., Champigny, G., Lazdunski, M., and Barbry, P. (1995) *Nature* **378,** 730–733
8. Canessa, C. M., Horisberger, J. D., and Rossier, B. C. (1993) *Nature* **361,** 467–470
9. Waldmann, R., Champigny, G., Bassilana, F., Heurteaux, C., and Lazdunski, M. (1997) *Nature* **386,** 173–177
10. Golubovic, A., Kuhn, A., Williamson, M., Kalbacher, H., Holstein, T. W., Grimmelikhuijzen, C. J., and Gründer, S. (2007) *J. Biol. Chem.* **282,** 35098–35103
11. Moosler, A., Rinehart, K. L., and Grimmelikhuijzen, C. J. P. (1996) *Biochem. Biophys. Res. Commun.* **229,** 596–602
12. Hansen, G. N., Williamson, M., and Grimmelikhuijzen, C. J. P. (2000) *Cell Tissue Res.* **301,** 245–253
13. Martinez, D. E., Dirksen, M. L., Bode, P. M., Jamrich, M., Steele, R. E., and Bode, H. R. (1997) *Dev. Biol.* **192,** 523–536
14. Paukert, M., Sidi, S., Russell, C., Siba, M., Wilson, S. W., Nicolson, T., and Gründer, S. (2004) *J. Biol. Chem.* **279,** 18783–18791
15. Chen, X., and Gründer, S. (2007) *J. Physiol.* **579,** 657–670
16. Canessa, C. M., Schild, L., Buell, G., Thorens, B., Gautschi, I., Horisberger, J. D., and Rossier, B. C. (1994) *Nature* **367,** 463–467
17. Loomis, W. F. (1955) *Ann. N. Y. Acad. Sci.* **62,** 211–227
18. Gonzales, E. B., Kawate, T., and Gouaux, E. (2009) *Nature* **460,** 599–604
19. Firsov, D., Schild, L., Gautschi, I., Mérillat, A. M., Schneeberger, E., and Rossier, B. C. (1996) *Proc. Natl. Acad. Sci. U.S.A.* **93,** 15370–15375
20. Hille, B. (2001) in *Ion Channels of Excitable Membranes*, 3rd Ed., pp. 471–502, Sinauer Associates, Inc., Sunderland, MA
21. Green, K. A., and Cottrell, G. A. (1999) *J. Physiol.* **519,** 47–56
22. Jeziorski, M. C., Green, K. A., Sommerville, J., and Cottrell, G. A. (2000) *J. Physiol.* **526,** 13–25
23. Green, K. A., and Cottrell, G. A. (2002) *Pflugers Arch.* **443,** 813–821
24. Meech, R. W., and Mackie, G. O. (1995) *J. Neurophysiol.* **74,** 1662–1670
25. Sakarya, O., Armstrong, K. A., Adamska, M., Adamski, M., Wang, I. F., Tidor, B., Degnan, B. M., Oakley, T. H., and Kosik, K. S. (2007) *PloS One* **2,** e506
26. Davey, F., Harris, S. J., and Cottrell, G. A. (2001) *J. Neurocytol.* **30,** 877–884
27. Cottrell, G. A., Green, K. A., and Davies, N. W. (1990) *Pflugers Arch.* **416,** 612–614
28. Palmer, L. G. (1997) *J. Gen. Physiol.* **109,** 675–676